Potential energy surface and unimolecular dynamics of stretched n-butane

Upakarasamy Lourderaj, Jason L. McAfee, and William L. Hase

Citation: The Journal of Chemical Physics **129**, 094701 (2008);
View online: https://doi.org/10.1063/1.2969898
View Table of Contents: http://aip.scitation.org/toc/jcp/129/9
Published by the American Institute of Physics

Potential energy surface and unimolecular dynamics of stretched *n*-butane

Upakarasamy Lourderaj, Jason L. McAfee, and William L. Hase[a)]
Department of Chemistry and Biochemistry, Texas Tech University, Lubbock, Texas 79409-1061, USA

(Received 15 May 2008; accepted 21 July 2008; published online 2 September 2008)

The potential energy surface (PES) and unimolecular reaction dynamics of stretched *n*-butane are investigated, as a model for a stretched "normal" alkane or straight chain polymer. The nature of the PES for stretched *n*-butane depends on the extent of stretching. If it is less than that required to reach the inflection points in the C—C stretch potentials and the C—C torsions are considered free rotors, there is only one potential energy minimum, with each bond elongated. However, for stretching past these inflection points, the PES has three minima and each has one bond longer than the other two, i.e., C—C—C—C, C—C—C—C, and C—C—C—C. There are three transition states (TSs) connecting these minima. A linear alkane, consisting of n carbon atoms and stretched past its C—C inflection points, has $(n-1)$ minima and $(n-1)(n-2)/2$ TSs connecting them. For stretching less than that required to reach the C—C inflection points, the only unimolecular pathways are dissociations to form the C+C—C—C, C—C+C—C, and C—C—C+C products. However, with stretching past the C—C inflection points, isomerizations between the three potential energy minima may also occur. The relative importance of isomerization versus dissociation depends on the relative size of their barriers. For slight stretching past the C—C inflection points, the isomerization barriers are much lower than those for dissociation and relaxation between the minima is much faster than dissociation. Thus, the molecule samples these minima randomly during its dissociation, with a density of states that comprises the complete PES. With extensive stretching past the inflection points, isomerizations between the potential energy minima do not occur and only dissociation for the excited minima occurs, e.g., C—C—C—C→C+C—C—C. For intermediate stretching past the C—C inflection points, the rates for the isomerization and dissociation pathways are competitive and both must be considered in modeling the dissociation kinetics. Microcanonical chemical dynamics simulations are performed to study the unimolecular kinetics of *n*-butane in three stretched configurations: Stretched less than the C—C inflection point; stretched slightly beyond the C—C inflection point; and stretched significantly beyond the C—C inflection point. The resulting unimolecular dynamics were found to be in excellent agreement with RRKM theory. Frequency ν factors, determined by fitting the trajectory unimolecular rate constants to the classical harmonic RRKM rate constant expression, depend upon the extent of stretching and vary from $1.0\times10^{12}-8.4\times10^{16}$ s^{-1}. For a molecule with a large number of vibrational degrees of freedom and high excess energy, it is shown that the classical harmonic RRKM and classical harmonic transition state theory rate constants, $k(E)$ and $k(T)$, are equivalent. © *2008 American Institute of Physics*. [DOI: 10.1063/1.2969898]

I. INTRODUCTION

Mechanical stress influences the manner in which molecules dissociate and undergo bimolecular reactions.[1] Stress affects properties of the reactive systems potential energy surface (PES), such as the potential energy barrier(s) for chemical reaction, and may alter the relative importance of different product channels as well as the reaction rate. In enzyme catalysis, potential energy barriers are lowered by mechanical stress.[2–5] Similar modifications of the reactants' PES have been suggested for tribochemistry occurring at sliding interfaces.[6,7]

There is considerable interest in understanding the atomic-level chemical dynamics of reactions under mechanical stress. Atomic force microscopy (AFM),[3] molecular dynamics simulations,[4] and nuclear magnetic relaxation (NMR) experiments[5] have probed the atomic-level motions associated with enzyme catalysis. Molecular dynamics simulations have been used to investigate the activation of titin kinase by mechanical stress.[8] The adsorption of macromolecules onto surfaces generates tensions within the molecules of sufficient strength to rupture covalent carbon-carbon bonds.[9,10] AFM experiments have investigated the activation of ligand substitution reactions by mechanical stress.[11] The application of mechanical stress has been used to activate and direct the course of ring opening chemical reactions.[12] A model energy landscape has been used to study the force-induced dissociation of ligand-receptor bonds.[13]

Computational studies provide an important means to determine how a chemical reaction's PES is modified in the presence of mechanical stress and the ensuing atomic-level chemical dynamics on this new PES. In this article such a study is presented of stretched *n*-butane as a model of a

a)Electronic mail: bill.hase@ttu.edu.

stretched "normal" alkane or straight chain polymer. The PES is first investigated as a function of the mechanical stress applied to the molecule. At a critical extent of stretching, the PES is found to undergo a transition from one with a single potential energy minimum to one with multiple minima and transition states. Properties of these minima and transition states are characterized. Chemical dynamics simulations[14,15] are performed to study how the unimolecular dynamics of stretched *n*-butane changes as the mechanical stress is increased. Of interest is the extent to which the unimolecular dynamics agrees with the random intramolecular vibrational energy redistribution (IVR) assumption[16] of Rice–Ramsperger–Kassel–Marcus (RRKM) theory,[17–19] the relative importance of C—C bond dissociation versus isomerization between multiple potential energy minima, and the frequency ν factors for the C—C dissociation reactions. In previous work,[20] comparisons were made between chemical dynamics simulations and RRKM theory in a study of the fragmentation of one-dimensional monoatomic chains under stress.

II. MODEL *n*-BUTANE POTENTIAL ENERGY FUNCTION

The model potential energy function used for *n*-butane is written as a sum of Morse stretches and attenuated harmonic bends, i.e.,

$$V = \sum_i D_i[1 - \exp\{-\beta_i(r_i - r_i^o)\}]^2 + \sum_k f_k(\theta_k - \theta_k^o)^2/2. \tag{1}$$

The force constant f_k is a function of the two bonds r_i and r_j, defining the bend angle θ_k, so that $f_k \rightarrow 0$ as either of the bonds ruptures, i.e.,

$$f_k(r_i, r_j) = f_\theta^o S(r_i) S(r_j). \tag{2}$$

The $S(r)$ are switching functions which attenuate f_θ^o and are written as[21]

$$S(r) = \begin{cases} 1, & \text{if } r < r^o \\ e^{-a(r-r^o)^2}, & \text{if otherwise} \end{cases}. \tag{3}$$

Values for r_i^o and θ_i^o were taken to match the experimental *n*-butane geometry.[22] Values for the stretching and bending force constants, i.e., f_r^o and f_θ^o, were taken from tabulated values for alkanes.[23] The bond energies D_i were taken from a recent compilation for organic molecules.[24] The Morse parameter β_i in Eq. (1) is related to D_i and f_r^o via the relationship $\beta = (f_r^o/2D)^{1/2}$. The r^o parameter in Eq. (3) is equated to the equilibrium bond length r_i^o and the parameter a to 1.00 Å^{-2}, a representative value for C—H and C—C bond elongation.[21]

For the unimolecular dissociation simulations reported here, the energy added to stretched *n*-butane is substantially larger than the 2–3 kcal/mol barriers for *n*-butane's internal rotation motions. Thus, the internal rotations of highly excited *n*-butane are well represented by free internal rotors and terms were not included in the potential energy function for the small internal rotation barriers. It is of interest that these barriers decrease as *n*-butane is stretched and this property could be investigated, in future work, by *ab initio* electronic structure calculations.

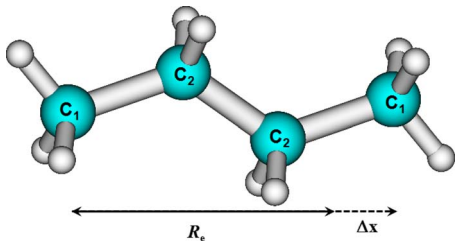

FIG. 1. (Color online) Model for stretched *n*-butane. The positions of the terminal carbon atoms are fixed. Their separation is 4.74 Å as compared to 3.91 Å for *n*-butane in its equilibrium geometry.

Using the subscripts 1 and 2 to identify, respectively, the primary atoms of the two terminal carbons and the secondary atoms of the two middle carbons, the following are the r_i^o, β_i, D_i, f_r^o parameters for each type of bond with respective units of Å, Å^{-1}, kcal/mol, and mdyne/Å: C_1—H_1, 1.1027, 1.829, 101.1, 4.699; C_2—H_2, 1.1055, 1.823, 98.6, 4.554; C_1—C_2, 1.5289, 1.883, 89.0, 4.387; and C_2—C_2, 1.5295, 1.884, 87.9, and 4.337. Similarly, the θ_k^o and f_k^o parameters, respectively, for each type of bend angle, in units of degrees and mdyne Å/rad^2, are H_1—C_1—H_1, 107.624, 0.540; H_1—C_1—C_2, 110.851, 0.645; H_2—C_2—C_1, 112.883, 0.656; H_2—C_2—C_2, 107.066, 0.656; H_2—C_2—H_2, 103.432, 0.550; and C_1—C_2—C_1, 112.851, 1.130.

III. POTENTIAL ENERGY SURFACE FOR STRETCHED *n*-BUTANE

To model *n*-butane under mechanical stress, it was stretched and then the positions of its two terminal carbon atoms were fixed in place, as shown in Fig. 1. The remaining atoms were allowed to move, when vibrational energy was added to the stretched molecule. The optimized geometry and vibrational frequencies of *n*-butane were determined for different amounts of mechanical stress. For the unstretched molecule the terminal carbon atoms are separated by 3.91 Å. As a mechanical stress is applied to the *n*-butane molecule and it is stretched, the structure of the global potential energy minimum changes and for some mechanical stresses there are multiple potential minima. Features of the *n*-butane potential energy surface, under mechanical stress, are discussed in the following.

A. Potential energy minima

An important property of the *n*-butane PES, under mechanical stress, is the inflection point in a C—C stretching potential. This point is located where the second derivative of the potential with respect to the stretching coordinate r_i equals zero and for the Morse potential in Eq. (1) is given by

$$r_i^{\text{inf}} = r_i^o + \frac{(\ln 2)}{\beta_i}. \tag{4}$$

Since β_i is slightly different for the C_1—C_2 and C_2—C_2 bonds, i.e., 1.883 and 1.884 Å^{-1}, the inflection points for these two types of C—C bonds occur at slightly different values of r_i. An additional important property of the PES for

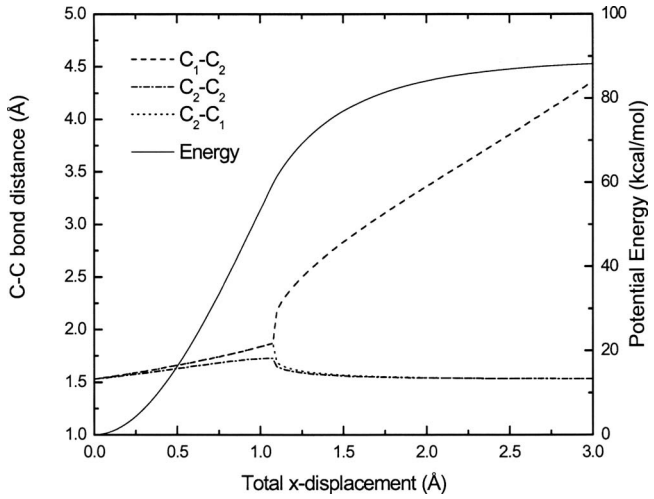

FIG. 2. Lengths (Å) of the three C—C bonds and the potential energy (kcal/mol) at the optimized geometry, with one terminal C_1—C_2 bond elongated for stretching past the C—C inflection point. The abscissa gives the total relative displacement of the terminal C_1–atoms along their x axis (see Fig. 1).

stretched *n*-butane is that, at equilibrium, the forces in each of the three C—C bonds are equal. The force for each C—C bond is found by taking the derivative of the bond's Morse function in Eq. (1) with respect to r_i, i.e., $\partial V(r_i)/\partial r_i$.

The number of potential energy minima on the stretched PES depends on whether the molecule has been stretched past an inflection point r_i^{inf}. The molecule *n*-butane, without stretching, has multiple potential energy minima arising from its three internal rotation (i.e., torsional) degrees of freedom. The barriers are low for transitions between these minima and, as discussed above, for the high energy simulations reported here the internal rotors are treated as free rotors. Thus, unstretched *n*-butane is modeled as having a single potential energy minimum. Of interest here is how the number of minima and shape of the PES change as *n*-butane is stretched. As the molecule is initially stretched there remains this single potential energy minimum, with each C—C bond stretched and equal forces in each C—C bond. However, once the molecule is stretched past the inflection point of any one of its C—C bonds, the PES has multiple potential energy minima. Up to this inflection point the C—C bonds are stretched nearly equivalently. However, once this point is passed for one of the bonds, its force starts to decrease and the lengths of the other two bonds begin to contract so that the forces in the three bonds remain equivalent. Since there are two equivalent C_1—C_2 bonds, there are two equivalent potential energy minima with one of these bonds stretched. There is also a potential energy minimum with the C_2—C_2 bond stretched and the other two C—C bonds contracted, to give three potential energy minima. Figure 2 gives the lengths of all three C—C bonds and the potential energy, at the equilibrium geometry for stretched *n*-butane, with the terminal C_1—C_2 bond elongated for stretching past the inflection points. The abscissa gives the total relative displacement of the terminal C_1 atoms (see Fig. 1). A similar figure results (not shown) with the middle C_2—C_2 bond elongated for stretching past the inflection point. Here, the two contracted C_1—C_2 bonds have the same length.

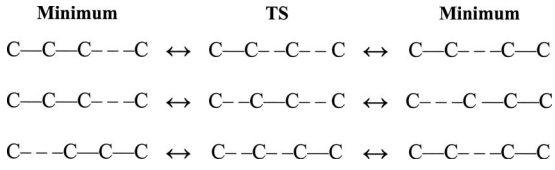

FIG. 3. Depiction of stretching for potential energy minima and TSs with $r > r^{\text{inf}}$.

As shown above, *n*-butane stretched past the inflection points, and with its torsions treated as free rotors, has three potential energy minima. In general, a linear alkane with n carbon atoms has $(n-1)$ potential energy minima, if its C—C bonds are stretched past their inflection points and its internal rotations are treated as free rotors. For each of these minima, one of the C—C bonds is longer than the remaining $(n-2)$, as discussed above. All the vibrational frequencies are real for these stationary points.

B. Isomerization transition states

Each of the three bonds may be stretched simultaneously beyond their inflection points, with an equivalent force in each bond. However, these are unstable stationary points, with two imaginary frequencies, and they will collapse into a lower energy stationary point if there is a minor perturbation for either one of the bonds. If each C_1—C_2 bond is compressed equivalently, at one of these unstable stationary points, to a length less than that for their inflection points, the system relaxes to a potential energy minimum with the C_2—C_2 bond elongated. On the other hand, if the C_2—C_2 bond is compressed to a distance shorter than its inflection point, the system relaxes to a structure with the two C_1—C_2 bonds elongated and the C_2—C_2 bond shortened. This stationary point has one imaginary frequency and corresponds to a transition state (TS) between the two potential energy minima for which only one C_1—C_2 bond is stretched (see Fig. 3). Similarly, there are TSs between the potential energy minimum with the C_2—C_2 bond stretched and the minima for one of the C_1—C_2 bonds stretched. For these stationary points, the C_2—C_2 bond and one of the C_1—C_2 bonds are elongated, with the other C_1—C_2 bond shortened. As for the equilibrium structures for the stretched molecule, the forces in the C—C bonds are equivalent at the TSs. Thus, for *n*-butane stretched beyond the C—C inflection points there are three TSs connecting the three potential energy minima. In general for a linear alkane with n carbon atoms, there are $(n-1)(n-2)/2$ TSs connecting the $(n-1)$ potential energy minima. There is only one imaginary frequency for each of these TSs.

The bond stretchings for the potential minima and their connecting TSs are depicted qualitatively in Fig. 3. Figure 4 gives the lengths (Å) of the three C—C bonds and the potential energy barrier (kcal/mol), versus stretching, for the transition state connecting the two potential energy minima with one C_1—C_2 bond stretched. The geometry of this TS smoothly connects with the geometry of the global potential energy minimum, with stretching less than that to reach the C—C inflection points. There is a similar figure (not shown) for the C—C—C—C TS connecting the C—C—C—C

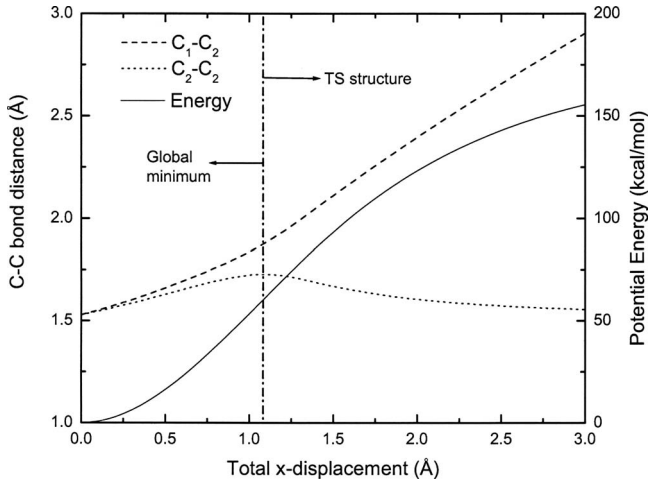

FIG. 4. Lengths (Å) of the three C—C bonds and the potential energy barrier (kcal/mol) for the transition state connecting the two potential energy minima with one C_1—C_2 bond stretched. These stationary points occur after the inflection point in the C_1—C_2 potential. The abscissa gives the total relative displacement of the terminal C_1 atoms along their x axis (see Fig. 1). The two terminal bonds, C_1—C_2 and C_2—C_1, have the same value for the global minimum and TS.

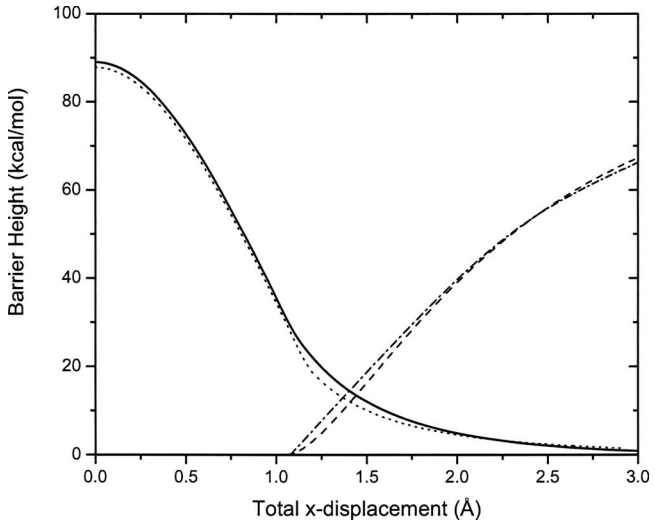

FIG. 6. Potential energy barriers for the C—C—C—C →C—C—C—C, –•–, and C—C—C—C→C—C—C—C, ----, isomerization pathways and pathways to form the C+C—C—C, —, and C—C+C—C, ⋯, products vs displacement of the terminal C_1 atoms.

and C—C—C—C minima. As in Fig. 4, the geometry of this TS also smoothly connects with the global potential energy minimum, with stretching less than that to reach the C—C inflection points. The potential energy minima and the isomerization TSs are illustrated by the contour diagram in Fig. 5.

C. Potential energy barriers

The potential energy barriers for C—C bond dissociation and isomerization between the potential energy minima vary as *n*-butane is stretched. The former decrease and the latter increase upon stretching. The values of these barriers, as a function of the stretching, are plotted in Fig. 6. For stretching of ~1.4 Å, the dissociation and isomerization barriers are approximately the same. Since the relative sizes of the dissociation and isomerization barrier are strongly dependent on the stretching of *n*-butane, one expects its unimolecular dissociation dynamics to depend on the stretching. This is illustrated and discussed in the Sec. IV.

D. Dissociation pathways

The dissociation pathways for *n*-butane with its terminal atoms fixed is substantially different from that for *n*-butane

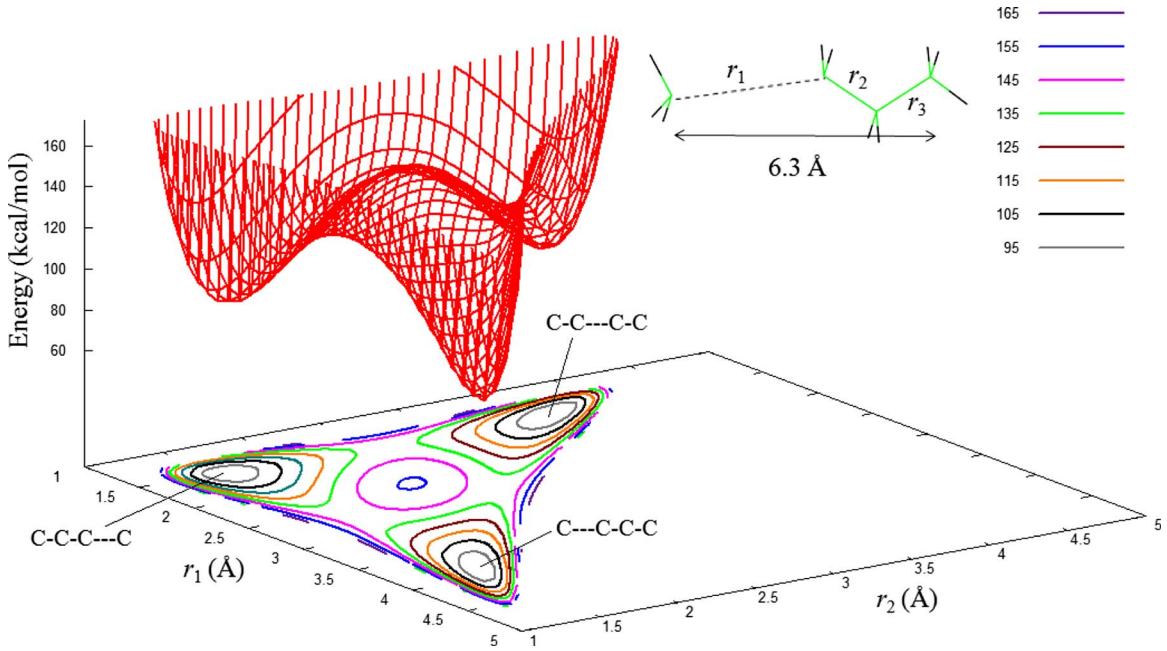

FIG. 5. (Color online) Two dimensional potential energy surface and contours for *n*-butane stretched extensively past the C—C inflection points, with the C_1 atoms displaced by 2.40 Å from the equilibrium separation of 3.9 Å. The structure at the top/right is for the C—C—C—C minimum. The numbers at the top/right define the energies (kcal/mol) for the contour lines.

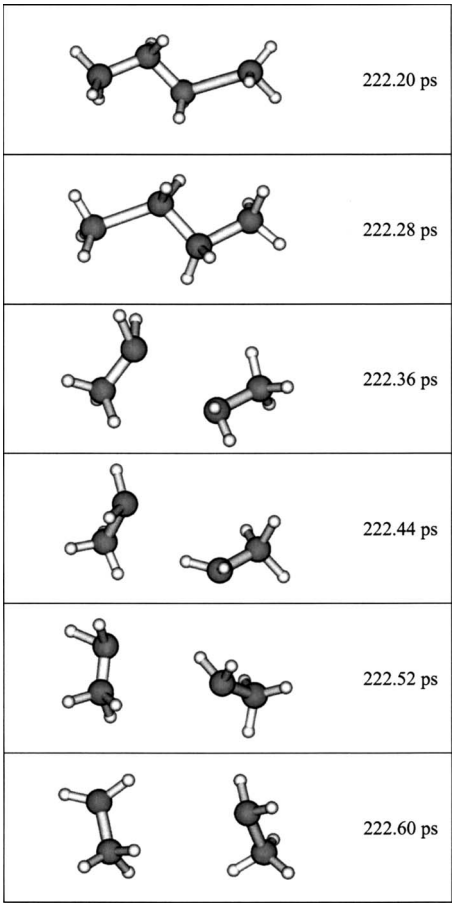

FIG. 7. Representative trajectory for a C—C bond dissociation pathway for *n*-butane stretched less than required to reach the inflection points and randomly excited in the single potential energy minimum.

in the gas phase. For the latter, dissociation occurs approximately along an axis connecting the two product C-atom radicals. However, with the terminal carbon atoms fixed, dissociation occurs by a motion approximately perpendicular to the axis connecting the two fixed C atoms. This is depicted in Fig. 7 for a trajectory dissociating by C_2—C_2 bond rupture. This trajectory is one of an ensemble of trajectories (discussed in the next section) randomly excited about the single potential energy minimum, with stretching less than needed to reach the C—C inflection points.

IV. UNIMOLECULAR DISSOCIATION DYNAMICS OF STRETCHED *n*-BUTANE

Chemical dynamics simulations were performed using the VENUS computer program,[25] as described previously,[14,15] to study the unimolecular dissociation of stretched *n*-butane. For a fixed stretching of *n*-butane, initial conditions for the trajectories were selected from a fixed energy microcanonical ensemble of states, using a modified microcanonical normal mode sampling scheme[26] as described in Appendix A. The trajectories were then calculated by numerically integrating Hamilton's equation of motion. The trajectories were integrated with a step size of 0.4 fs for a maximum of 1 ns. Each trajectory dissociated by C—C bond rupture within this interval. Energy was conserved to within 0.001 kcal/mol.

The lifetime, for C—C bond dissociation of stretched *n*-butane, is the time a transition from an excited *n*-butane molecule to products occurs. A specific C—C bond length was used to identify this transition and lengths in the range of 5–6 Å were found to be appropriate and gave the same result. Trajectories attaining this C—C bond extension went on to form products. For shorter bond lengths as a criterion for dissociation, some of the trajectories immediately returned and reformed excited stretched *n*-butane. The specific criterion to identify C—C bond dissociation was a length of 5 Å.

In the following, chemical dynamics simulations are reported for the unimolecular decomposition of microcanonical ensembles of states for stretched *n*-butane. Three different extensions of *n*-butane are considered to study the unimolecular dynamics in three different stretching regions. The simulation results are compared with the predictions of RRKM unimolecular rate theory. As shown in Appendix B, for a large excitation energy E and for the relatively large number, $s=36$, of vibrational modes of stretched *n*-butane, the microcanonical RRKM $k(E)$ and canonical transition state theory (TST) $k(T)$ become equivalent with $E=sk_BT$.

A. Stretching to the C—C inflection points

As discussed above, for *n*-butane stretched less than that required to reach the C—C inflection points, the potential energy surface has only one potential energy minimum and the microcanonical ensemble of states is sampled about this minimum. The rate constant for this initial microcanonical ensemble, i.e.,

$$k_{\mathrm{RRKM}} = -\frac{1}{N(0)}\frac{dN(t)}{dt}\bigg|_{t=0} \tag{5}$$

is the microcanonical unimolecular rate constant of RRKM theory.[14,15] The assumption of RRKM theory is one of rapid intramolecular vibrational energy redistribution (IVR), on the time scale of the unimolecular dissociation,[16] so that a microcanonical ensemble is maintained throughout the dissociation.[14,15,26] As a result, the RRKM dissociation probability versus time is

$$P(t) = -\frac{1}{N(0)}\frac{dN(t)}{dt}\bigg| = k_{\mathrm{RRKM}}\exp(-k_{\mathrm{RRKM}}t), \tag{6}$$

where both the initial dissociation probability and the decay of $P(t)$ are specified by $k_{\mathrm{RRKM}}=k(E)$, where E is the energy of stretched *n*-butane in excess of its potential energy minimum. Non-RRKM unimolecular dynamics are identified by an exponential rate constant different than k_{RRKM} or nonexponential unimolecular decay.[14,27]

A unimolecular chemical dynamics simulation, as described above, was performed for *n*-butane stretched with 39.2 kcal/mol potential energy. With this stretching potential, *n*-butane is stretched 0.825 Å and short of the inflection point, as shown in Fig. 2. Thus, it has one minimum with a potential energy of 39.2 kcal/mol. An excess energy of 130 kcal/mol is added to this minimum, which corresponds

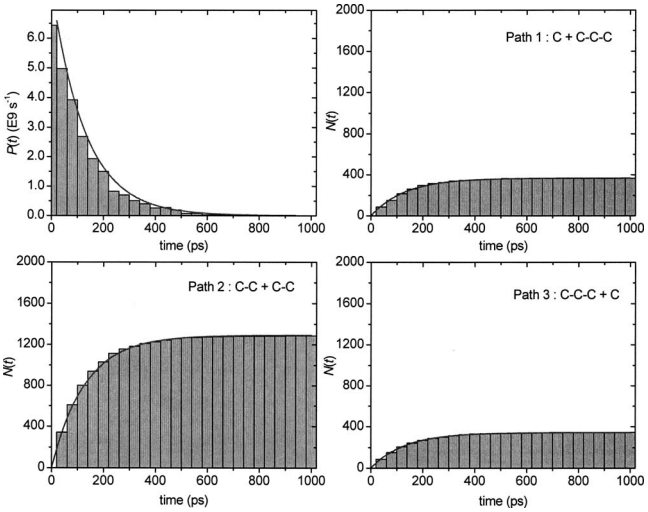

FIG. 8. Simulation results for *n*-butane stretched less than that required to reach the C—C inflection points. Stretching potential is 39.2 kcal/mol, displacement of the C_1 atoms is 0.825 Å, and excess energy is 130 kcal/mol. $P(t)$ for stretched *n*-butane and total number of product molecules versus time, $N(t)$, are given for paths 1, 2, and 3. These distributions are well fit by RRKM theory.

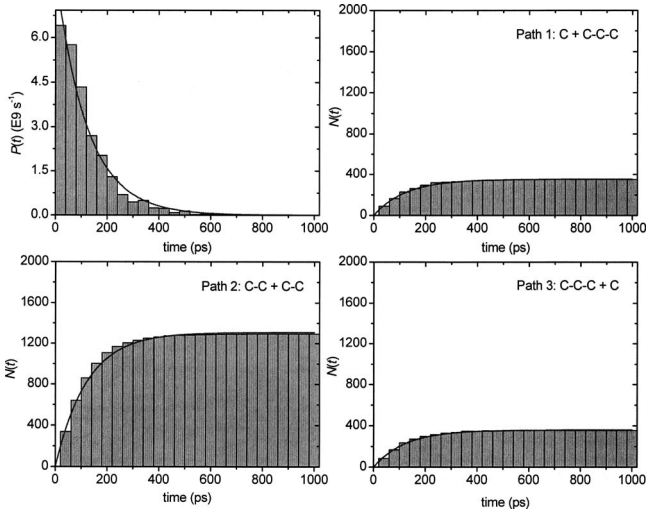

FIG. 9. Simulation results for *n*-butane stretched slightly past the inflection points. The stretching potential is 62.9 kcal/mol, displacement of the C_1 atoms is 1.125 Å, and excess energy is 70 kcal/mol. $P(t)$ for stretched *n*-butane and total number of product molecules vs time, $N(t)$, are given for paths 1, 2, and 3. These distributions are well fit by RRKM theory.

to a temperature of 1817 K, i.e., $E=36k_BT$. The resulting $P(t)$, Eq. (6), and the total number of products versus time, $N(t)$, for each of the three product channels,

$$\begin{aligned} \mathrm{C-C-C-C} \rightarrow\ & \mathrm{C+C-C-C}, \quad \text{path 1} \\ & \mathrm{C-C+C-C}, \quad \text{path 2} \\ & \mathrm{C-C-C+C}, \quad \text{path 3}, \end{aligned}$$

are plotted in Fig. 8. $P(t)$ agrees with the exponential form of RRKM theory and is fit by the rate constant $7.7\pm0.1\times10^9$ s^{-1}. The rate constants for paths 1, 2, and 3 were determined by fitting the populations versus time using $k_{\mathrm{RRKM}}=7.7\times10^9$ s^{-1} and the values are 1.4×10^9, 5.0×10^9, and 1.3×10^9 s^{-1}, respectively. They sum to 7.7×10^9 s^{-1}, the same as the k that fits $P(t)$. In addition, the rate constants for paths 1 and 2 differ by only 7%. These unimolecular kinetics agree with the prediction of RRKM theory.

The RRKM unimolecular rate constant for a specific reaction path is

$$k_{\mathrm{RRKM}}=\frac{1}{h}\frac{N^{\neq}(E-E_o)}{\rho(E)}, \tag{7}$$

where $N^{\neq}(E-E_o)$ is the sum of states for the reaction path's transition state (TS) and $\rho(E)$ is the density of states for the decomposing molecule. If the vibrational modes are assumed to be harmonic, the classical RRKM rate constant is given by Eq. (B2), see Appendix B. Using the C—C dissociation barriers of 48.7 kcal/mol for path 2 and 49.8 kcal/mol for paths 1 and 3, the above trajectory rate constants may be fit with Eq. (B2), to give a frequency factor ν of 6.8×10^{16} s^{-1} for path 2 and 3.0×10^{16} s^{-1} for paths 1 and 3. As shown by Eq. (B9), the ν factors may include an anharmonic correction factor. In addition, these C—C bond dissociation TSs are expected to be variational[28,29] and will, thus, have a potential energy E_o less than that of the C—C bond dissociation energy. This will have the effect of decreasing the fitted ν factor.

B. Stretching slightly past the C—C inflection points

A microcanonical unimolecular dynamics simulations was also performed for *n*-butane only stretched slightly past the C—C inflection points. *n*-butane was stretched 1.125 Å with a potential energy of 62.9 kcal/mol. As shown in Fig. 6, for this stretching, the barriers for isomerization between the potential energy minima are much lower than those for C—C bond dissociation and rapid equilibrium between the minima is expected on the time-scale for dissociation. This is indeed found to be the case. Figure 9 illustrates the result of a simulation with the C—C—C—C potential energy minimum excited randomly with 70 kcal/mol of excess energy, $T=978$ K. There is no indication of *apparent* non-RRKM behavior,[14] as a result of the initial non-random excitation and the dissociation appears completely random. Thus, the analysis of the simulation results is the same as that given above for a single potential energy minimum. $P(t)$ in the figure is for dissociation by all three pathways, and is exponential and fit by $k_{\mathrm{RRKM}}=8.2\pm0.3\times10^9$ s^{-1}. Rate constants for pathways 1, 2, and 3 were determined by fitting their populations $N(t)$, using the above k_{RRKM}. The resulting respective rate constants are 1.4×10^9, 5.4×10^9, and 1.5×10^9 s^{-1}, which sum to 8.3×10^9 s^{-1}, nearly the same as the fitted k_{RRKM}. The rate constants for paths 1 and 3 are nearly the same, which should be the case, with the one for path 3 slightly larger, even though the minimum for path 1, C—C—C—C, was excited. The kinetics is RRKM, with rapid equilibration of the minima.[30]

The expression for the RRKM rate constant for each of the dissociation paths is the same as that given by Eq. (7), except the density of states, $\rho(E)$, now represents that for all three minima, which are randomly occupied. An approximate representation of $\rho(E)$ is to write it as a sum of the

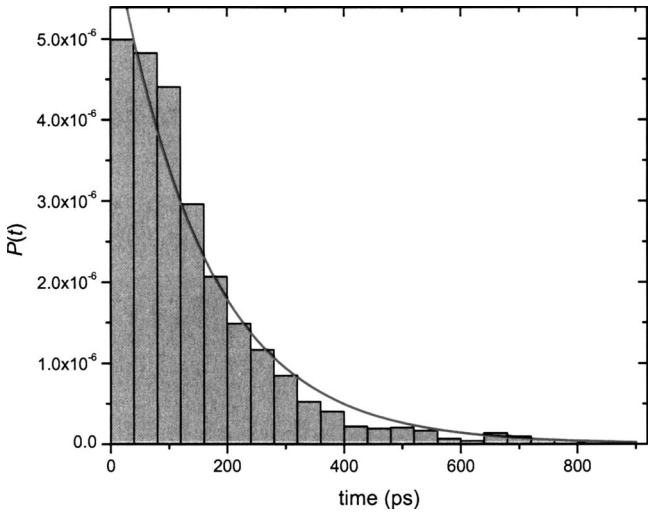

FIG. 10. Simulation results for *n*-butane stretched extensively past the C—C inflection points with a stretching potential of 86.3 kcal/mol and 2.35 Å displacement of the C_1–atoms. The C—C—C—C minimum was excited randomly with 20 kcal/mol and only C—C—C—C→C+C—C—C dissociation occurred. The resulting $P(t)$ is fit with RRKM theory.

density of states for the three minima, i.e., $\rho(E)=\rho_1(E)+\rho_2(E)+\rho_3(E)$.[30] Since, as shown in Fig. 6, the dissociation energies are similar for rupturing the C_1—C_2 and C_2—C_2 bonds, $\rho(E)\sim 3\rho_1(E)$. Thus, the classical harmonic RRKM rate constant may be approximated by Eq. (B2) divided by 3. Using this approximation the ν factor is 8.4×10^{16} s^{-1} for path 2 and 5.4×10^{16} s^{-1} for paths 1 and 3.

C. Stretching extensively past the C—C inflection points

A unimolecular dynamics simulation was performed, as described above, with *n*-butane stretched to a potential energy of 86.3 kcal/mol, so that the two terminal carbon atoms were displaced 2.35 Å with respect to the *n*-butane equilibrium geometry. For this stretching, the C—C dissociation barriers are low and the isomerization barriers are much higher, as shown in Fig. 6. A microcanonical ensemble of states was sampled about the C—C—C—C potential energy minimum with an excess energy of 20 kcal/mol, which corresponds to a temperature of 280 K. As a result of the high barriers for transitions between the potential energy minima, there were no isomerizations and only dissociation to form the C+C—C—C products occurred. $P(t)$ for dissociation of stretched *n*-butane is exponential, as shown in Fig. 10, with a rate constant of $6.4\pm0.3\times10^9$ s^{-1}. Inserting the C—C dissociation energy of 2.7 kcal/mol for E_o into Eq. (B2) yields a ν factor of 1.0×10^{12} s^{-1}. For this dissociation, k_{RRKM} is the rate constant for dissociation via path 1 and is given by Eq. (7). The density of states is that for the C—C—C—C potential energy minimum.[12]

V. SUMMARY

For the study presented here, the following results were obtained concerning the PES and unimolecular dynamics of *n*-butane stretched under mechanical stress:

(1) To determine properties of the *n*-butane PES in the presence of mechanical stress, *n*-butane is elongated by displacing its terminal carbon atoms a fixed distance. The resulting topology of *n*-butane's PES depends on the extent of this stretching. If it is less than that required to reach the inflection points in the C—C stretch potentials, there is only one potential energy minimum, with each bond elongated. However, for stretching past the inflection points, these structures are no longer minima, but unstable fixed points.[31] With this stretching, the PES acquires three minima and each has one bond longer than the other two, i.e., C—C—C—C, C—C—C—C, and C—C—C—C. There are three TSs connecting these minima. A linear alkane, consisting of n carbon atoms and stretched past its C—C inflection points, has $(n-1)$ minima and $(n-1)(n-2)/2$ TSs connecting them.

(2) For stretching less than that required to reach the C—C inflection points, the only unimolecular pathways are dissociations to form the C+C—C—C, C—C+C—C, and C—C—C+C products. However, with stretching past the C—C inflection points, there are isomerization pathways between the three potential energy minima. The relative importance of isomerization versus dissociation depends on the relative size of their barriers. For stretching slightly past the C—C inflection points, the isomerization barriers are much lower than those for dissociation and the molecule randomly samples the three minima during its dissociation. With stretching extensively past the inflection points, the isomerization barriers are large and only dissociation for the excited minima occurs, e.g., C—C—C—C→C+C—C—C. For intermediate stretching past the C—C inflection points, the rates for the isomerization and dissociation pathways are competitive.

(3) Microcanonical chemical dynamics simulations show that the unimolecular dissociation of stretched *n*-butane is *intrinsically* RRKM.[14] The harmonic RRKM ν factors, determined from the simulation rate constants, are four orders of magnitude smaller for *n*-butane stretched extensively past the inflection points as compared to those for stretching less than needed to reach the C—C inflection points and for stretching slightly past the inflection points. There appear to be two contributing factors to this effect. Only four rocking-type vibrational frequencies change in moving from the potential energy minimum of stretched *n*-butane to the dissociation TS and, thus, the ν factor in Eq. (B2) may be approximated by $\nu\sim\nu_{st}(\Pi_{i=1}^4\nu_{r,i}/\Pi_{i=1}^4\nu_{r,i}^{\neq})$. Here, ν_{st} is the frequency of the potential minimum's C—C stretch, which becomes the reaction coordinate, and the $\nu_{r,i}$ and $\nu_{r,i}^{\neq}$ are the rocking vibrational frequencies for the stretched potential minimum and the dissociation TS, respectively. The value for ν_{st} decreases as the molecule is stretched and, since $\nu_{r,i}$ decreases upon stretching, the $\nu_{r,i}/\nu_{r,i}^{\neq}$ ratio is also expected to decrease with stretching. Both of these factors will cause the ν factor to decrease as *n*-butane is stretched. Inconsistent with this argument are the ν factors, for stretching slightly past the C—C

inflection points, which are 1.2 and 1.8 times larger than those for stretching less than that required to reach the C—C inflection points. To accurately understand this effect, it may be necessary to (1) represent the density of states more accurately, than is done here (Sec. IV B) for the random sampling of the three potential energy minima with slight stretching past the C—C inflection points; and (2) determine the ν factors versus excess energy as well as the stretching and mechanical stress (see discussion below).

For the future, several important extensions of the current study are possible. By performing microcanonical chemical dynamics simulations versus energy for different extensions of stretched *n*-butane, the RRKM ν-factors may be determined versus energy and the mechanical stress. The possible importance of this information is discussed above. In addition, it should be possible to calculate the intrinsic reaction coordinates (IRCs) (Ref. 32) for the dissociation of stretched *n*-butane and the vibrational frequencies as functions of the IRCs.[33,34] With this information, variational TSs (Ref. 28 and 29) can be determined for the C—C dissociation reactions and the harmonic RRKM rate constants, Eq. (B4), may be calculated. They may be compared with the microcanonical (i.e., anharmonic RRKM, Ref. 35) rate constants determined from the chemical dynamics simulations, to determine the anharmonic components, Eq. (B9), in the ν factors. For simulations performed with intermediate stretching, where isomerizations and dissociations are competitive, analyses of the chemical dynamics simulations will provide anharmonic RRKM rate constants for both the isomerization and dissociation reactions. Comparing them with the harmonic RRKM rate constants will give anharmonic corrections for both dissociation and isomerization. Finally, it would be of interest to extend these studies to macromolecules, e.g., biomolecules, to investigate the nature of their PESs and unimolecular dynamics under mechanical stress.

ACKNOWLEDGMENTS

The research here is based upon work supported by the Office of Naval Research under Grant No. N00014-04-1-0366, the National Science Foundation under Grant No. CHE-0615321, and the Robert A. Welch Foundation under Grant No. D-0005. The authors wish to thank Dr. Robert Shroll for suggestions concerning the modified microcanonical normal mode sampling algorithm.

APPENDIX A: MODIFIED ALGORITHM FOR MICROCANONICAL NORMAL MODE SAMPLING

Classical microcanonical normal-mode sampling[14,36] considers a molecule consisting of n normal modes at a constant total energy E. The probability that normal mode 1 has energy E_1 is proportional to the number of ways the energy $E-E_1$ may be added to the remaining $n-1$ oscillators. This is given by the density of states for these oscillators; thus, the normalized probability that normal mode 1 contains energy E_1 is

$$P(E_1) = (E-E_1)^{n-2}\left(\int_0^E (E-E_1)^{n-2} dE_1\right)^{-1}. \tag{A1}$$

The general expression for the probability that oscillator i has energy E_i is

$$P(E_i) = \left(E - \sum_{j=1}^{i-1} E_j - E_i\right)^{n-1-i} \times \left\{\int \left(E - \sum_{j=1}^{i-1} E_j - E_i\right)^{n-1-i} dE_i\right\}^{-1}. \tag{A2}$$

Equation (A2) is conveniently sampled using a cumulative distribution function[37] to give for the individual E_i,

$$E_i = \left(E - \sum_{j=1}^{i-1} E_j\right)(1 - R_i^{1/(n-i)}), \tag{A3}$$

where R_i represents a freshly generated random number ranging between 0 and 1. Each E_i is then transformed to a normal mode coordinate Q_i and momentum P_i, by choosing a random phase for the normal mode.[15,38,39]

The normal-mode eigenvector is then used to transform the Q_i and P_i to the Cartesian coordinates q_i and momenta p_i, which are used to integrate the classical trajectory. Since normal modes are approximate for finite displacements, the energy calculated from the Cartesian q_i and p_i will differ from the intended energy, given by the normal modes. Usually this difference is quite small and the following are some average differences between the Cartesian and intended normal mode energies, i.e., zero-point energy (ZPE) in C_2H_4, 0.1%;[40] ZPE in benzene, 4.0%;[41] and zpe and 300 K thermal energy in the $[Cl{=}CH_3{=}Cl]^-$ transition state, 3.8%.[42] Since this difference is small, the Cartesian displacement coordinates and momenta are scaled until the Cartesian energy and intended normal mode energy agree to within 0.1%. This scaling is not severe and at most usually only one or two scalings are required.

There are two situations for which the above sampling scheme does not work and must be modified so that only kinetic energy is added to a particular mode, i.e., the transformation between normal mode and Cartesian kinetic energies is exact.[43] One is for internal rotational degrees of freedom which are free or nearly free rotors,[44] as is the case here for the *n*-butane model with three free rotors. The other is for very low frequency vibrational modes for which the displacements of the Cartesian coordinates is quite extensive and, thus, the normal mode to Cartesian coordinate transformation is inexact and problematic. This has been discussed previously[45] for the low frequency intermolecular modes of the Cl^-—CH_3Br ion-dipole complex. This was also found to be a problem here for the low frequency C—C stretching and C—C—C bending modes of stretched *n*-butane. To correct this problem and obtain accurate microcanonical sampling, as illustrated by Figs. 8–10, the following modification was made to the classical microcanonical normal mode sampling algorithm of Ref. 36:

(1) The normal modes are arranged by ascending vibrational frequencies;

(2) Both kinetic and potential energy are added to each normal mode, via a random phase, as described above;
(3) The normal mode Q_i and P_i are transformed to Cartesian q_i and p_i and the Cartesian energy calculated.

If it agrees to within 10% with the intended normal mode energy, the Cartesian Δq_i and p_i are scaled and the initial condition is accepted. If not, only kinetic energy is added to the lowest frequency normal mode, which in the above step had both kinetic and potential energy. The procedure loops back to step 3. If the resulting Cartesian and normal mode energies do not agree within 10%, the procedure again loops back to step 3 and so forth.

For the unimolecular simulations of stretched *n*-butane presented here, on average only kinetic energy was added to eight modes for stretching less than the C—C inflection points, to 5 modes for slight stretching past the C—C inflection points, and to eight modes for extensive stretching past the inflection points. Butane has 36 normal modes and, of the above modes with only kinetic energy, three are the C—C free rotors for the *n*-butane model used here.

APPENDIX B: RELATIONSHIP BETWEEN CLASSICAL HARMONIC RRKM AND TST THEORIES

For classical mechanical unimolecular decomposition, the harmonic microcanonical (RRKM), and canonical (transition state theory, TST) unimolecular rate constants become the same at high energy and for a molecule with a large number of vibrational modes s. The RRKM, $k(E)$, and TST, $k(T)$, are related by[46]

$$k(T) = \frac{1}{Q_r}\int k(E)\rho(E)e^{-E/k_BT}dE, \tag{B1}$$

where $\rho(E)$ is the density of states of the reactant molecule and Q_r its partition function. For classical unimolecular decomposition, the harmonic RRKM rate constant is[19]

$$k(E) = \frac{\Pi_{i=1}^{s}\nu_i}{\Pi_{i=1}^{s-1}\nu_i^{\neq}}\left(\frac{E-E_o}{E}\right)^{s-1} = \nu\left(\frac{E-E_o}{E}\right)^{s-1}, \tag{B2}$$

where the ν_i are the vibrational frequencies for the molecule, the $\nu_i^{\neq}$ the vibrational frequencies for the transition state (TS), and E_o the classical potential energy barrier for unimolecular decomposition. The classical harmonic TST rate constant is given by

$$k(T) = \frac{k_BT}{h}\frac{\Pi_{i=1}^{s-1}q_i^{\neq}}{\Pi_{i=1}^{s}q_i}e^{-E_o/k_BT}, \tag{B3}$$

where the $q_i^{\neq}$ and q_i are the individual vibrational partition functions for the TS and the molecule, respectively. Inserting the expressions for $q_i^{\neq}$ and q_i (i.e., $q_i=k_BT/h\nu_i$) into Eq. (B3) yields

$$k(T) = \nu e^{-E_o/k_BT}, \tag{B4}$$

where the ν factor is the same as in Eq. (B2).

For large E and large s the above $k(E)$ and $k(T)$ become the same. To begin write

$$\ln k(E) = \ln \nu + (s-1)\ln(1-E_o/E). \tag{B5}$$

For large E and small E_o/E, one has

$$\ln(1-E_o/E) = -E_o/E. \tag{B6}$$

Also, for classical vibrations,

$$\langle E\rangle = sk_BT. \tag{B7}$$

Setting E to $\langle E\rangle$, and inserting Eqs. (B6) and (B7) into Eq. (B5), one finds that

$$\ln k(T) = \ln \nu - \frac{(s-1)}{s}\frac{E_o}{k_BT}. \tag{B8}$$

For $s\approx(s-1)$, Eq. (B8) becomes the TST expression in Eq. (B4).

If an anharmonic correction factor, f_{anh}, is introduced,[35] the RRKM rate constant becomes

$$k_{\text{anh}}(E) = f_{\text{anh}}(E)\nu\left(\frac{E-E_o}{E}\right)^{s-1}. \tag{B9}$$

The above relationship shows that, for large E and large s, the canonical rate constant is

$$k(T) = f_{\text{anh}}(T)\nu e^{-E_o/k_BT}. \tag{B10}$$

[1] M. K. Beyer and H. Clausen-Schauman, Chem. Rev. (Washington, D.C.) **105**, 2921 (2005).
[2] A. Fersht, *Structure and Mechanism in Protein Science* (Freeman, New York, 1999).
[3] A. P. Wiita, R. Perez-Jimenez, K. A. Walther, F. Gräter, B. J. Berne, A. Holmgren, J. M. Sanchez-Reuiz, and J. M. Fernandez, Nature (London) **450**, 124 (2007).
[4] K. A. Henzler-Wildman, V. Thai, M. Lei *et al.*, Nature (London) **450**, 838 (2007).
[5] K. A. Henzler-Wildman, M. Lei, V. Thai, S. J. Kerns, M. Karplus, and D. J. Kern, Nature (London) **450**, 913 (2007).
[6] M. Akbulut, A. R. Godfrey Alig, and J. Israelachvili, J. Chem. Phys. **124**, 174703 (2007).
[7] M. Koyama, J. Hayakawa, T. Onodera, K. Ito, H. Tsuboi, A. Endou, M. Kubo, C. A. Del Carpic, and A. Miyamoto, J. Phys. Chem. B **110**, 17507 (2006).
[8] F. Gräter, J. Shen, H. Jiang, M. Gautel, and H. Grubmüller, Biophys. J. **88**, 790 (2005).
[9] S. Granick and S. C. Bae, Nature (London) **440**, 160 (2006).
[10] S. S. Sheiko, F. C. Sun, A. Randall, D. Shirvanyants, M. Rubinstein, H.-il. Lee, and K. Matyjaszweski, Nature (London) **440**, 191 (2006).
[11] F. R. Kersey, W. C. Yount, and S. L. Craig, J. Am. Chem. Soc. **128**, 3886 (2006).
[12] B. M. Rosen and V. Percec, Nature (London) **446**, 381 (2007); C. R. Hickenboth, J. S. Moore, S. R. White, N. R. Sottos, J. Baudry, and S. R. Wilson, *ibid.* **446**, 423 (2007).
[13] T. Strunz, K. Oroszlan, I. Schumakovitch, H.-J. Güntherodt, and M. Hegner, Biophys. J. **79**, 1206 (2000).
[14] D. L. Bunker and W. L. Hase, J. Chem. Phys. **59**, 4621 (1973).
[15] G. H. Peslherbe, H. Wang, and W. L. Hase, Adv. Chem. Phys. **105**, 171 (1991).
[16] W. L. Hase, J. Phys. Chem. **90**, 365 (1986).
[17] R. A. Marcus and O. K. Rice, J. Phys. Colloid Chem. **55**, 894 (1951).
[18] H. M. Rosenstock, M. B. Wallenstein, A. L. Wahrhaftig, and H. Erying, Proc. Natl. Acad. Sci. U.S.A. **38**, 667 (1952).
[19] T. Baer and W. L. Hase, *Unimolecular Reaction Dynamics. Theory and Experiments* (Oxford University Press, New York, 1996).
[20] K. Bolton, S. Nordholm, and H. W. Schranz, J. Phys. Chem. **99**, 2477 (1995).
[21] R. J. Wolf, D. S. Bhatia, and W. L. Hase, Chem. Phys. Lett. **132**, 493 (1986).
[22] NIST Computational Chemistry Comparison and Benchmark Database, NIST Standard Reference Database Number 101, Release 14 Sept. 2006,

edited by R. D. Johnson III, http://srdata.nist.gov/cccbdb
[23] S. Califano, *Vibrational States* (Wiley, New York, 1976).
[24] Y.-R. Luo, *Handbook of Bond Dissociation Energies in Organic Compounds* (CRC, Boca Raton, FL, 2003).
[25] W. L. Hase, R. J. Duchovic, X. Hu, A. Komornicki, K. F. Lim, D. -H. Lu, G. H. Peslherbe, K. N. Swamy, S. R. Vande Linde, L. Zhu, A. Varandas, H. Wang, and R. J. Wolf, *Quantum Chemistry Program Exchange (QCPE) Bulletin* 16, 671 (1996).
[26] D. L. Bunker, J. Chem. Phys. **40**, 1946 (1964).
[27] W. L. Hase, D. G. Buckowski, and K. N. Swamy, J. Phys. Chem. **87**, 2754 (1983).
[28] W. L. Hase, J. Chem. Phys. **64**, 2442 (1976).
[29] W. L. Hase, Acc. Chem. Res. **16**, 258 (1983).
[30] Reference 19, p. 270.
[31] A. J. Lichtenberg and M. A. Liberman, *Regular and Chaotic Dyamics*, 2nd ed. (Springer-Verlag, New York, 1991), p. 49.
[32] K. Fukui, J. Phys. Chem. **74**, 4161 (1970).
[33] W. H. Miller, N. C. Handy, and J. E. Adams, J. Chem. Phys. **79**, 6046 (1983).
[34] W. L. Hase and R. J. Duchovic, J. Chem. Phys. **83**, 3448 (1985).
[35] K. Song and W. L. Hase, J. Chem. Phys. **110**, 6198 (1999).
[36] W. L. Hase and D. G. Buckowski, Chem. Phys. Lett. **74**, 284 (1980).
[37] D. L. Bunker, Methods Comput. Phys. **10**, 287 (1971).
[38] S. Chapman and D. L. Bunker, J. Chem. Phys. **62**, 2890 (1975).
[39] C. S. Sloane and W. L. Hase, J. Chem. Phys. **66**, 1523 (1977).
[40] W. L. Hase, D. M. Ludlow, R. J. Wolf, and T. Schlick, J. Phys. Chem. **85**, 958 (1981).
[41] D.-h. Lu and W. L. Hase, J. Chem. Phys. **91**, 7490 (1989).
[42] Y. J. Cho, S. R. Vande Linde, L. Zhu, and W. L. Hase, J. Chem. Phys. **96**, 8275 (1992).
[43] S. Califano, *Vibrational States* (Wiley, New York, 1976), pp. 23–26.
[44] N. Davidson, *Statistical Mechanics* (McGraw-Hill, New York, 1962), pp. 199–200.
[45] G. H. Peslherbe, H. Wang, and W. L. Hase, J. Am. Chem. Soc. **118**, 2257 (1996).
[46] J. I. Steinfeld, J. S. Francisco, and W. L. Hase, *Chemical Kinetics and Dynamics* (Prentice-Hall, Upper Saddle River, NJ, 1999).